Original Article Open Access

Archives Of Breast Cancer

DOI: 10.32768/abc.2024112159-171

Acquisition of Doxorubicin Resistance Induces Breast Cancer Cell Migration and Epithelial-Mesenchymal Transition that are Reversed by Shikonin-Metformin Synergy

Atlas Keshandehghan[§a], Abolfazl Rostamian Tabari[§a], Yasin Panahi[b], Mossa Gardaneh*[a,c]

[a]*National Institute of Genetic Engineering and Biotechnology, Tehran, Iran*

[b]*Department of Basic Medical Sciences, Khoy University of Medical Sciences, Khoy, Iran*

[c]*Genomedicx Co., Richmond Hill, Ontario, Canada*

[§]These authors have contributed equally to this study

ARTICLE INFO

Received:
13 February2024
Revised:
14 April 2024
Accepted:
15 April 2024

Keywords:
breast cancer, drug resistance, doxorubicin, shikonin, metformin

ABSTRACT

Background: Drug resistance is a major challenge in cancer chemotherapy.

Methods: By adopting an appropriately timed strategy, we generated MCF-7 cell sublines resistant to serial doses of doxorubicin (DOX). Our higher-dose sublines showed more stability in resistance and were, therefore, subjected to further analyses. We tested the consistency of drug resistance by comparing sublines with control groups for growth and migration capacities. Molecular analyses monitored expression changes, CD44/CD24 ratios, and DOX binding to key molecules. The reverting impact of shikonin (SHKN) and metformin (MTFN) on DOX resistance was examined.

Results. The resistant sublines grew parallel to or even faster than WT MCF-7 cells and showed a larger and more rounded morphology. The consistency of their drug resistance and invasive potential was demonstrated over time using serial doses of DOX. Real-time PCR revealed upregulation of genes involved in cell growth and survival, drug resistance, migration/invasion, and epithelial-mesenchymal transition and, conversely, downregulation of pro-apoptotic, anti-chemoresistance, and tumor suppressor genes. SHKN-MTFN co-treated resistant cells showed significantly lower CD44/CD24 ratios, less aggressiveness, and reduced survival and migration rates but enhanced apoptosis. SHKN's affinity to CYP1A and TOP2A demonstrated the importance of these interactions and the compounds' capacity to compete with DOX.

Conclusion: Acquisition of DOX resistance increases tumorigenic properties of cancer cells, whereas synergy between selective anti-tumorigenic compounds re-sensitizes resistant cells by reverting cellular pathways that favor or follow resistance. Our findings suggest that this reversal is supported by competing reactions that deprive DOX of binding to its target molecules.

Copyright © 2024. This is an open-access article distributed under the terms of the Creative Commons Attribution-Non-Commercial 4.0 International License, which permits copy and redistribution of the material in any medium or format or adapt, remix, transform, and build upon the material for any purpose, except for commercial purposes.

***Address for correspondence:**
Mossa Gardaneh
National Institute of Genetic Engineering and Biotechnology, Pazhoohesh Blvd, Tehran-Karaj HWY Kilometer 15, PO BOX 14965/161, Tehran-Iran
Tel:+982144580344
Email: mossa65@nigeb.ac.ir; mossabenis65@gmail.com

INTRODUCTION

Drug resistance (DR) in cancer is developed, regulated, and balanced by multiple determinants that include environmental and intrinsic factors besides treatment pressures.[1] Molecular mechanisms by which these determinants promote cancer DR are diverse and span from drug-receptor

Breast cancer (BC) chemotherapy frequently ends up with DR which may confer a more aggressive nature to patient tumors. Doxorubicin (DOX; Adriamycin) is a natural anthracycline used to treat solid and blood tumors.[3] DOX is broadly considered the most effective single drug available for the treatment of BC.[3,4] The compound damages cancer cells by intercalating into DNA, thereby disrupting topoisomerase-II (TOP2)-mediated DNA repair, and destroying cellular membranes by generating free radicals.[5] A combination of anthracyclines such as DOX and taxanes has produced the most desirable disease-free and/or overall survival in BC patients.[6]

DOX therapy, on the other hand, is capable of inducing DR that leads to tumor growth and eventually poor patient prognosis and survival.[7] Despite several efforts to remedy it, DOX resistance remains a major unresolved issue in BC therapy. Multiple mechanisms, including reduced intracellular DOX concentrations caused by overexpressed membrane efflux pumps, increased drug-metabolizing enzymes, reduced concentrations and activity of TOP2A, and deregulated intracellular apoptotic pathways, are the main causes of DOX resistance.[7,8]

Some reports are available that outline modeling DOX resistance in BC and other cancer types *in vitro* and *in vivo*. They include cell lines of breast and colorectal cancers[9-12] and a murine model of BC.[7] These studies indicate profound morphological, molecular, and behavioral changes in resistant tumor models that need to be taken into consideration when searching for effective solutions to DOX resistance.

We have been studying DR in BC for some time and have created trastuzumab-resistant models of BC tumor xenografts for molecular analyses.[13] In the current study, we generated MCF-7 cell sublines resistant to various doses of DOX and examined some changes that occur in the course of resistance acquisition. We then tested our notion that a combination of the anti-tumorigenic compound shikonin (SHKN) and anti-diabetic metformin (MTFN) could effectively remedy resistance and induce apoptotic cell death.

METHODS

Cell culture and chemicals

Human BC cell line MCF-7 was obtained from the National Cell Bank of Pasture Institute (Tehran, Iran), cultured in Dulbecco's modified eagle's medium (DMEM; Gibco, 12430054) supplemented with 10% fetal calf serum (FBS; Gibco, A4766801), and maintained at 37 °C and 5% CO2. Shikonin was purchased from Sigma (54952-43-10) and dissolved in dimethyl sulfoxide (DMSO; Thermo Fisher, 20688). Metformin was gifted by Dr. Abidi Co (Tehran) and dissolved in PBS to form treatment stocks.

Drug treatment

Doxorubicin Hydrochloride (DOX.Hcl) was dissolved in DMSO (2mg/ml) to prepare initial stocks. MCF-7 cells were split 24 hrs before setting up any experiment involving the cells. About 15000 cells/well were seeded in a 96-well plate. After 24 hrs of growth, the cells were treated with serial concentrations of DOX stocks prepared beforehand from 1 to 2500 nanomolar (nM). The cells were re-incubated for another 24 hrs before adding the MTT solution and being subjected to the viability assay for IC_{50} determination. This experiment was repeated three times and, parallel to the drug, the same volumes of DMSO, a DOX solvent, were applied to the treatment/viability assay.

MTT viability assay and IC50 determination

MTT viability was done as a standard method. Briefly, MCF-7 cells were treated with serial concentrations of DOX in 96-well plates. DMSO, PBS (drugs' solvents), and untreated cells were used in parallel as our base controls. After a 24-hr incubation period, we exposed the cells to the MTT (Sigma, M5655) solution to measure viability. In the end, we read the absorbance at 580 nm using an ELISA reader. The calculated inhibitory concentrations (IC_{50}s) represent the treatment concentrations that inhibit 50% of cells' growth versus controls.

Test of resistance continuity

The strategy to generate DOX-resistant sublines is outlined in the Results section. To make sure of resistance continuity, we treated the cells with both specific doses of DOX and serial concentrations of the drug, before examining viability.

Cell migration assay

The scratch assay was used to assess migration. Wild-type MCF-7 cells and resistant sublines were seeded in 6-well plates (4×10^5 cells per well) to become 80% confluent in 24 hrs and ready for drug treatment. The next day, a sterile razor blade was used to scrape cells off the culture plate, leaving a denuded area and a sharp visible demarcation line at the wound edge. The wounded monolayers were gently washed with PBS twice and inspected under phase-contrast microscopy immediately after wounding. Then, sections of the wounds were selected according to the criteria and numbered. The photographs collected from cell samples were trimmed and edited so that they would more closely represent the migration process. Migrated cells were counted in sections 500

μm in length, allowing a 20 μm space from the scratch line to minimize the possible physical effects of cell movement resulting from cell proliferation. Statistical analysis was calculated by averaging a mean of six sections per test for each experiment. The number of migrated cells was expressed as mean±SEM. We repeated these experiments trice in each group to ensure reproducibility.

Cell co-staining and live-cell count

Acridine orange (AO) co-applied with ethidium bromide (EB) stains nuclear DNA green in live cells and orange in dead cells. We followed our standard AO/EB co-staining method to measure the percentage of viable treated MCF-7 cells. Briefly, 50-μL suspension of each cell group was mixed with 50 μL of the pre-made stain stock and subjected to counting under fluorescent light. Six random microscopic fields per well were selected to count an average of 120 cells for each cell group in triplicates (three wells per group), as we have reported.[13]

Flow cytometric analysis of stem cell surface markers CD24 and CD44

Suspensions of untreated cell samples and those treated for 24 hrs were incubated with fluorochrome-conjugated antibodies (1:1) against human CD24 (PE-conjugated) (Thermo Fisher, 12-0242-82) and CD44 (FITC-conjugated) (Thermo Fisher, 11-0441-82) at 4°C in dark for 30–40 min and detected in the FL2/PE channel. The labeled cells were analyzed by flow cytometry.

RNA extraction and Real-time qPCR assay

RNA extraction and cDNA synthesis were done as we have described.[13] Each reaction included template cDNA, gene-specific primers, and SYBRGreen I PCR Master Mix. The human GAPDH was used as an internal control. All data were normalized to the expressed human GAPDH gene and alterations of expression were measured using the delta-delta Ct method.[14] Table 1 shows the primers used for our reactions.

Table 1. Primer Sequences for Real-time PCR

	Name	Primer Sequence	Size (bp)	Accession #
1	CDH1	F *AGGCCAAGCAGCAGTACATT* R *ATTCACATCCAGCACATCCA*	110	NM_001317185.2
2	SNAIL1	F *TCGGAAGCCTAACTACAGCGA* R *AGATGAGCATTGGCAGCGAG*	140	NM_005985.4
3	STAT3	F *CAGCAGCTTGACACACGGTA* R *AAACACCAAAGTGGCATGTGA*	150	NM_001384993.1
4	P21	F *AGACCAGCATGACAGATTTC* R *ACTGAGACTAAGGCAGAAGA*	144	NM_001220777.2
5	TOP2A	F *TGTGATTAGTGGTGAAGTAGC* R *AGTGGTATCTGTATGGTATTCC*	175	NM_001067.4
6	BCL2	F *GTGGCCTTCTTTGAGTTCG* R *CCCAGCCTCCGTTATCCT*	145	NM_000657.3
7	BAX	F *TGGAGCTGCAGAGGATGATTG* R *GAAGTTGCCGTCAGAAAACATG*	170	NM_138761.4
8	P53	F *TCAACAAGATGTTTTGCCAACTG* R *ATGTGCTGTGACTGCTTGTAGATG*	118	NM_001126118.2
9	GAPDH	F *GAGTCCACTGGCGTCTTCAC* R *GTTCACACCCATGACGAACA*	120	NM_001357943.2
10	ABCB1	F *TTCCTTCAGGGTTTCACATTTG* R *TTAACTTGAGCAGCATCATTGG*	167	NM_001348945.2
11	ABCC1	F *CTGATGGAGGCTGACAAGGC* R *AAGGAAGATGCTGAGGAAGGA*	105	NM_004996.4
12	BRCA2	F *GCCAGAGATATACAGGATATGCG* R *TATGAGAACACGCAGAGGGA*	154	NM_000059.4
13	CYP1A1	F *TTCTCCATTGCCTCTGACCCA* R *ACTGATACCACCACATACCTGT*	149	NM_000499.5
14	CCND1	F *GCTGCGAAGTGGAAACCATC* R *CCTCCTTCTGCACACATTTGAA*	135	NM_053056.3
15	PI3K	F *TTCTCCATATTAGATTTACCCACAG* R *TGATTCTTTCAAAAGGAACAACATT*	102	NM_181524.2
16	AKT1	F *CACCGTGTGACCATGAATGAG* R *TTCTCCTTGACCAGGATCACC*	83	NM_001382431.1
17	MMP9	F *TTGACAGCGACAAGAAGTGG* R *GCCATTCACGTCGTCCTTAT*	179	NM_004994.3

Molecular docking

The structure of DOX and shikonin were taken, respectively, from these sites: www.zinc15.docking.rg, and https://pubchem.ncbi.nlm.nih.gov/. Autodock Vina software was used to examine molecular interactions in an *in-silico* environment. The software was also applied for final analyses and binding energy measurement, as we have reported.[15] Finally, Discovery Studio Visualization (DSV) was applied to visualize 2D and 3D binding structures.

Statistical analysis

The results are presented as mean ± SE. Statistical comparisons between groups were carried out using one-way ANOVA followed by the Student's t-test. We used the data of triplicates or more repetitions for each set of experiments, and comparisons were carried out only between relevant pairs of data. We considered a value of $P<0.05$ as statistically significant, and $P<0.01$ or $P<0.001$ as highly significant.

RESULTS

Our strategy to generate DOX-resistant MCF-7 sublines

First, we treated WT MCF-7 cells with serial concentrations of DOX and measured cell viability (Figure 1A). We determined 1 µM as the IC_{50} of DOX. To begin with our strategy, we split the WT cells and, 24 hrs after, treated them using 5% of the DOX IC_{50} for a few weeks until they adapted to the drug (Figure 1B). We split the cells again, preserved a fraction as our first MCF-7 subline named 5%, and maintained the second half in a drug-free medium for one week. This time, we split these cells and treated them with 5% of the drug IC_{50} for 24 hrs, followed by a second dose (10%) for a few weeks for adaptation and generation of the second subline that was named 10%. We repeated these cycles of treatment, adaptation, and drug-free growth until sublines of 15%, 20%, and 25% were generated. Morphologically, there were no major differences between various sublines and their ancestral WT cells when we observed them under the phase-contrast microscope (Figure 1C). We found the sublines at lower doses (5-15%) unstable in the long term as they started decreasing in number and perishing after several times of splitting. In comparison, the 20% and particularly 25% sublines showed long-term stability that provided a reasonable time window for us to subject them to further experimentation. In addition, our attempt to generate 30% and beyond faced failure as the cells did not survive to adapt to higher DOX concentrations. Because of their reasonable stability, the 25% subline was most relied upon for our subsequent analyses.

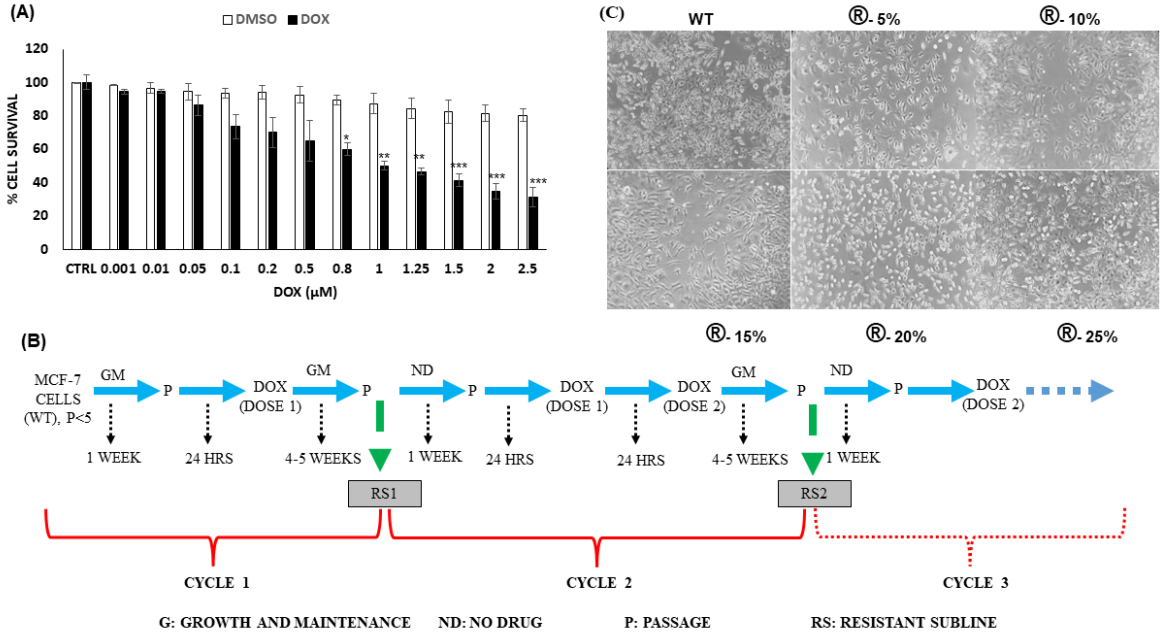

Figure 1. Generation of doxorubicin-resistant sublines: **a)** Viability of WT MCF-7 cells treated with serial concentrations of doxorubicin. Each column represents the average of three independent experiments that included triplicate wells of cells in 96-well plates for each DOX concentration. As a control, the same volumes of DMSO as the DOX solvent were applied. These data were applied to normalize the data of DOX- and shikonin-treated cells in all subsequent graphs of cell growth. Symbol *, **, *** represent statistical differences between each DOX treatment with its DMSO control. **b)** A strategy to generate resistant sublines. **c)** Morphology of a number of isolated resistant sublines.

Generated MCF-7 sublines show resistance to DOX

To test if our sublines maintain their DOX-resistant property, we first grew them in a medium that contained their dose of DOX for a few days. Next, we split the cells and seeded them in equal numbers in 96-well plates, incubated them with and without DOX for 24 hrs, and tested their viability using MTT. In our control (no drug) group, both 20% and 25% resistant sublines showed comparable viability to our WT cells (Figure 2A). Treatment with 20% of the drug IC_{50} slowed down viability in WT cells to some extent (non-significant) but failed to do so in our 20% and 25% sublines. The 25% dose of the IC_{50} slightly reduced viability in WT and the 20% subline but not in our 25% subline (Figure 2A). These observations indicate that the sublines maintained their growth and stability when exposed to their dose of drug concentrations. Next, we measured cell viability by treating our sublines with serial concentrations of DOX. We found that while there is a sharp decline in WT cell survival, this decline is slowed down in our resistant sublines (Figure 2B). Our last test was on the migrating capacity of the two sublines (Fig. 2C). Numerical measurement based on the counting of the number of cells crossing the scratch line indicated our 20% and 25% sublines preserve their potential to migrate, and, the 25% even does significantly better than both WT control and the 20% subline (Figure 2D; P<0.05).

FIG. 2

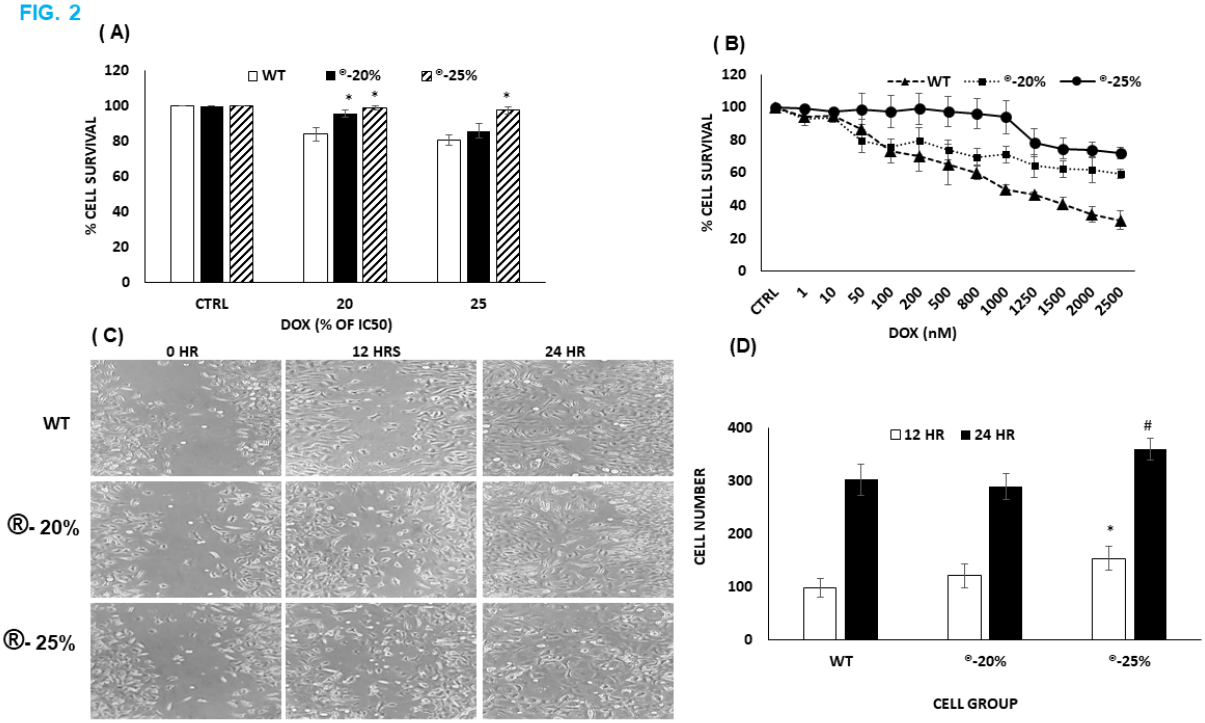

Figure 2. Doxorubicin resistance in generated MCF-7 sublines: **a)** Compared to WT cells: each column represents a subline treated with the same percent of IC_{50}: subline 20% and treated with 20% dox, and subline 25% treated with 25% dox. **b)** Changes in growth rate of resistant sublines compared to the WT MCF-7 cells. **c)** Preserved capacity of the resistant sublines to migrate, compared to the WT MCF-7. **d)** Numerical representation of changes in cell migration capacity. Each column represents an average of three independent experiments. Symbol * shows statistical differences in migration between 12-hr sample (R-25%) and control (WT).

MCF-7 sublines undergo pro-resistance and pro-EMT changes at molecular levels

Once we ensured our generated sublines maintained their DOX resistance capacity, we monitored three classes of molecular changes as post-resistance acquisition in our 25% subline. Firstly, real-time experiments revealed upregulated genes that included cell cycle gene CCND1, growth signaling genes PI3K and AKT1, ABCB1, and ABCC1, and CYP1A1, anti-apoptosis gene BCL-2, pro-migration genes SNAIL, STAT3 and MMP1 (Figure 3A and Table 2). CYP1A1 showed the most significant upregulation (by 105 folds; P<0.01, compared to the WT MCF-7), while others had a 3 to 14 folds increase in their mRNA expression. In contrast, these genes were downregulated: pro-apoptosis genes BAX, p53, anti-migration gene CDH1, anti-chemoresistant gene TOP2A, and tumor suppressors BRCA2 and p21. The most notable reduction was observed in the expression of TOP2A (by 102 folds; P<0.01), followed by CDH1 (21 folds; P<0.01).

Table 2. Fold increases and decreases in mRNA levels of gene candidates shown by real-time PCR

GENE	FOLD INCREASE
CYP1A1	106
ABCB1	12.7
ABCC1	8.7
PI3K	5.4
AKT1	4.34
BCL-2	3.69
SNAIL	14.1
STAT3	7.25
MMP1	3.7
CCND1	6.62
TOP2A	-103
BRCA2	-18
P21	-1.2
BAX	-1.7
P53	-3.2
CDH1	-21

Our second class of molecular studies examined virtual binding between DOX and a number of these molecules. In particular, DOX binding to CYP1A1 and TOP2A was evaluated (Figure 3B). We detected strong binding energies: -8.4 between DOX and TOP2A and -7.5 between DOX and CYP1A1. We have already published the images of binding between DOX and key molecules of intracellular signaling pathways.[15] The energies of these bindings are listed in Table 3.

Due to the importance of CSCs in cancer DR, we devoted our third class of molecular studies to changes in stem cell markers in our resistant 25% subline. Figure 3.C shows over 120% increase in the CD44/CD24 ratio in our resistant subline compared to its WT ancestor (P<0.05).

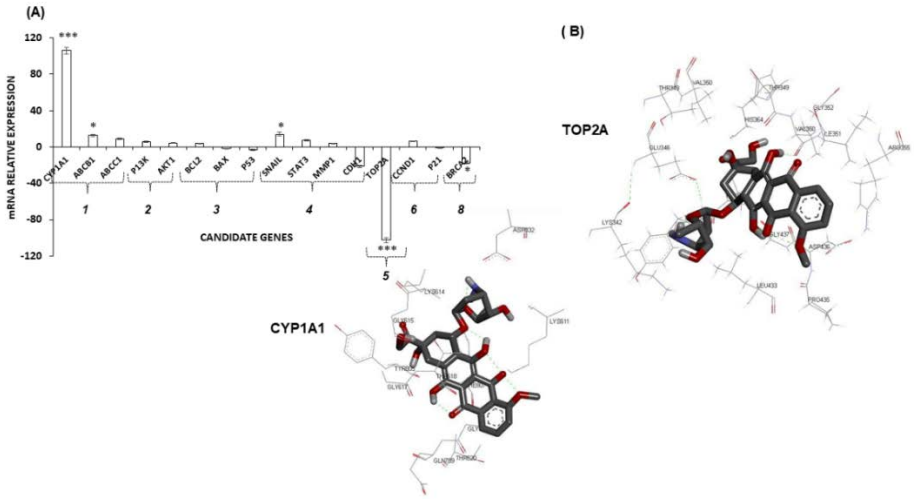

Figure 3. Molecular changes in resistant sublines: **a)** Changes in mRNA expression levels of some key molecules measured by quantitative real-time PCR. Each column represents an average of three independent experiments. Symbols * and *** represent, respectively, significant and highly significant differences in gene expression between the 25% resistant subline the and WT MCF-7 cells. **b)** A diagram representing binding between doxorubicin and key molecules TOP2A, and CYP101, generated by the molecular docking software, as outlined in our previous study.[15] **c)** The ratio of stem cell markers CD44:CD24 in resistant subline compared to WT MCF-7.

Table 3. Binding energies between drugs and cellular molecules**.** Figures of binding energies for growth pathway molecules were borrowed from our previous study [17].

DOX Affinity (KCal/Mol) to drug resistance molecules					
CYP1A1	TOP2A				
-7.5	-8.4				
SHKN Affinity (KCal/Mol) to drug resistance					
CYP1A1	TOP2A				
-6.4	-6.7				
SHKN Affinity (KCal/Mol) to PI3K/AKT Pathway					
PI3Kα	PI3Kγ	PI3Kδ	AKT1	AKT2	mTOR
-7.7	-7.9	-7.4	-7.6	-7.8	-7.8
SHKN Affinity (KCal/Mol) to MAPK/ERK Pathway					
HRAS	RAF1	MEK1	MEK2	ERK1	ERK2
-8.4	-6.2	-8	-8.3	-8.7	-8.6

SHKN-MTFN synergy reverses DOX resistance and halts aggressive behavior

Based on our previous observations on the impact of SHKN-MTFN synergy on the inhibition of cancer cell migration and reversal of EMT,[15] we examined the impact of the combination on our resistant sublines. Applying a similar range of doses, we determined IC_{50} of SHKN to be 10 µM for WT MCF-7, 12 µM for our 20% subline, and 15 µM for our 25% subline (Table 4). The figures for MTFN stood, respectively, at 60, 68, and 75 mM. Based on our previous report,[15] we used the RSM method and determined these IC_{50} doses for SHKN-MTFN co-treatment: 7 µM /40 mM for WT MCF-7, 9 µM /45 mM for our 20% subline, and 11 µM /52 mM for our 25% subline (see Table 4).

Table 4. IC_{50} of shikonin and metformin in wild-type MCF-7 and its resistant sublines

	SHKN (µM)	MTFN (mM)	SHKN-MTFN
WT	10	60	7&40
R-20%	12	68	9&45
R-25%	15	75	11&52

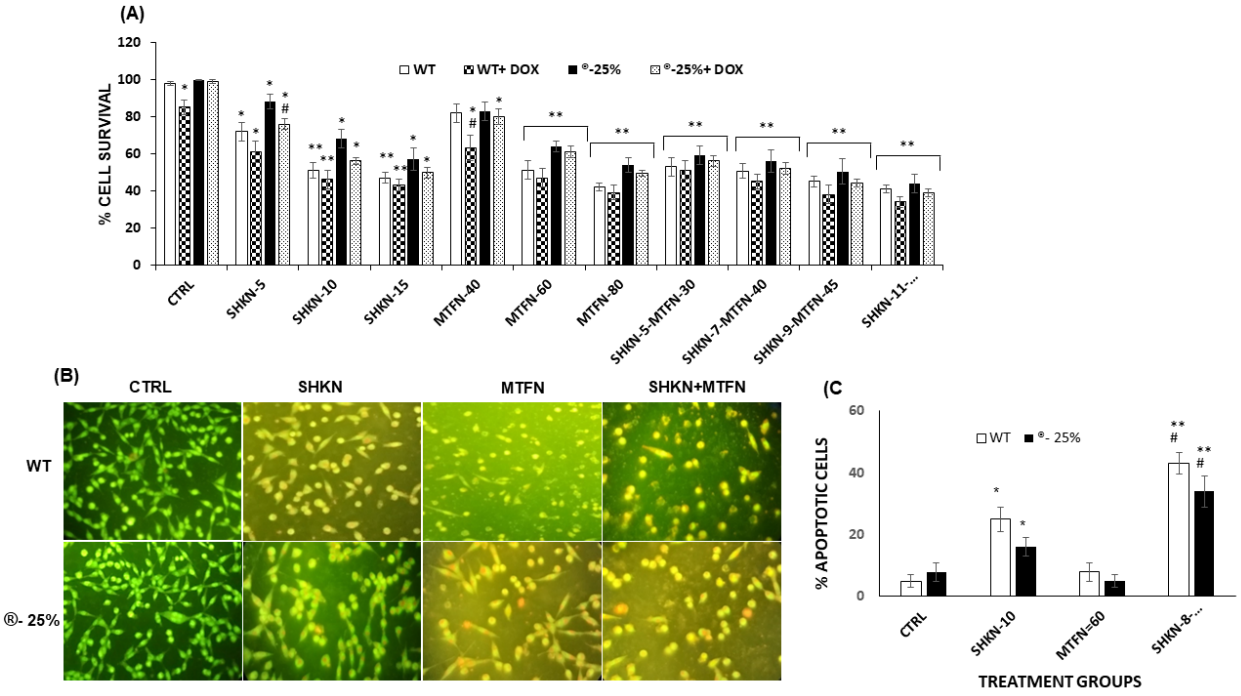

Figure 4. Resistance break by SHKN-MTFN combination: **a)** Reduced survival induced by SHKN-MTFN combination; **b)** Enhanced apoptosis induced by SHKN-MTFN treatment; **c)** Numerical measurement of apoptosis post-treatment

Figure 4A shows that, compared to the untreated WT MCF-7 cells, increasing concentrations of SHKN and MTFN in separation significantly reduce cell survival. This trend emerged in our resistant 25% subline as well. When we used the two compounds in their sublethal doses, similar or lower levels of cell viability were detected in both WT and resistant cell groups. In particular, WT cells showed significantly reduced levels of viability when treated with DOX IC_{50} ($P<0.05$). However, the resistant subline was not affected by 25% of the IC_{50} dose, indicating its ongoing adaptation to the drug. Our SHKN-MTFN co-treated samples showed similar levels of viability to their single-treated counterparts, which were further and significantly reduced when higher doses of the combination drugs were applied (Figure 4A). We also examined the impact of SHKN-MTFN synergy on cell apoptosis (Figure 4B) and found that the combined treatment significantly induces cell death compared to WT cells (Figure 4C; $P<0.01$) and single treatments ($P<0.05$).

SHKN-MTFN synergy promotes migration inhibition in resistant subline

We then tested the capacity of SHKN-MTFN synergy to inhibit subline migration. This potential of our 25% subline was reduced dramatically by single treatments (Figure 5A,B). Numerical counting of the cells crossing the scratch line determined more reduction in cell number with increasing SHKN or MTFN dosage and in 24 hrs post-scratch compared to 12 hrs (Figure 5C). Co-treatment with both compounds (Figure 5C) significantly reduced the number of migrating cells compared to both WT and single-treated cell groups (Figure 5D; $P<0.01$).

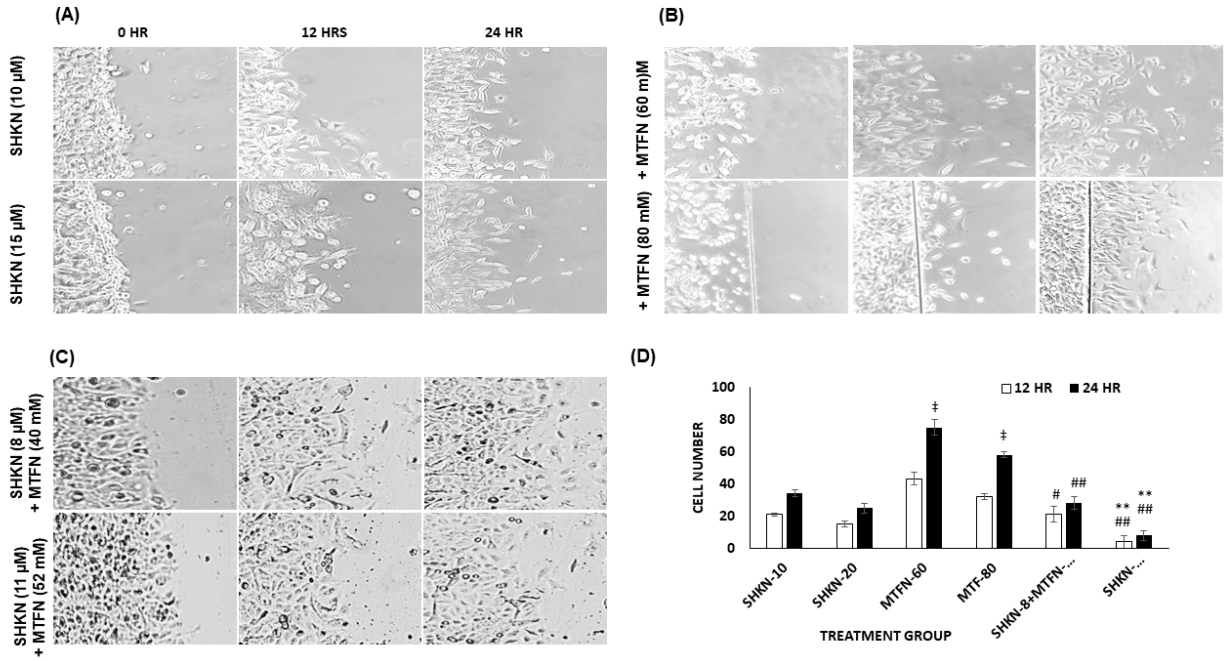

Figure 5. Migration inhibition of resistant subline: R-25% treated with (a) SHKN, (b) MTFN and (c) both. Magnification: 20x. Graph (d) numerically summarizes the changes. The horizontal axis shows treatment groups and the vertical axis shows the average number of cells that have crossed the scratch line after 12 and 24 hrs. Each column was generated by counting crossing the scratch line and representing the average of three independent experiments. * is a symbol of significant differences between SHKN-MTFN and SHKN treatments, whereas # represents differences between SHKN-MTFN and MTFN treatments and ‡ compares 24-hr and 12-hr migrating groups.

SHKN-MTFN synergy promotes molecular changes to reverse drug resistance

We examined molecular changes that might occur upon treatment and co-treatment of our resistant subline with SHKN and MTFN. We looked at the changes in CD44/CD24 ratios in treated samples. Table 5 summarizes these changes. As reported before,[15] treatments with SHKN, and to some extent MTFN, significantly reduced the CD44/CD24 ratio in WT MCF-7 ($P<0.01$). Likewise, the increasing concentrations of either drug significantly reduced the ratio in our resistant 25% subline (Table 5; SHKN $P<0.01$; MTFN $P<0.05$). Similar to the synergistic impact of SHKN-MTFN co-treatment on MCF-7 cell tumorigenicity,[15] co-treatment using various sub-lethal concentrations of the compounds also reduced the ratio in our 25% subline. These reductions were highly significant compared to our single treatments (see Table 5 for comparisons and significance of changes).

Table 5. The significant impact of SHKN-MTFN co-treatment on stem cell markers ratio

#	Sample	CD44:CD24 Ratio	Comments
1	MCF-7 (WT)	394	
2	®- 25%	485*	Induced vs #1
3	WT + SHKN (12 µM)	63 ***	Highly reduced vs #1
4	WT + MTFN (60 mM)	132*	Reduced vs #1
5	WT + MTFN (80 mM)	111**	Highly reduced vs #1
6	®- 25% + SHKN (12 µM)	94.5 ##	Highly reduced vs 2
7	®- 25% + SHKN (15 µM)	50 ###	Highly reduced vs 2
8	®- 25% + SHKN (20 µM)	37 ###	Highly reduced vs 2
9	®- 25% + MTFN (60 mM)	190 #	Reduced vs 2
10	®- 25% + SHKN (9 µM) + MTFN (45 mM)	46 ###	Highly reduced vs 2 & 6
11	®- 25% + SHKN (11 µM) + MTFN (45 mM)	33 ###	Highly reduced vs 2 & 6
12	®- 25% + SHKN (11 µM) + MTFN (52 mM)	29 ###	Highly reduced vs 2 & 6

In our previous study, we showed a strong binding between SHKN and several key molecules involved in BC cell growth and survival.[15] Based on the role of SHKN in inhibiting DR, migration, and EMT observed in the current study, we further examined SHKN binding to two key more molecules that showed profound changes in their expression: CYP1A1 and TOP2A. The binding energy of SHKN was determined to be -6.4 KCal/Mol for CYP101 and -6.7 KCal/Mol for TOP2A. There is no fixed baseline for ligand-receptor binding, but based on different investigators' comments on the world wide web, we took -6 Kcal/Mol and below as a sign of strong binding. Table 3 lists the binding energies.

DISCUSSION

Doxorubicin is currently the most effective single chemo-drug for BC therapy. However, treated tumors often face DOX resistance that ends up in tumor recurrence and poor patient prognosis. In general, intra-tumoral heterogeneity and clonal evolution that stem from somatic mutations and genomic plasticity during tumor development form the foundations of cancer DR including DOX resistance.[16] These changes are fueled by interactions between signaling pathways that induce proliferation, cell cycle progression and apoptosis inhibition.[1,7] Our study was aimed at dissecting some details of mechanisms behind DOX resistance and examining the notion that shikonin-metformin synergy can restore cancer cell responsiveness.

In order to generate our resistant sublines, we designed and adopted a strategy based on which DOX doses beginning with 5% of IC_{50} and increasing in increments were applied for cell treatment. We also applied phases of treatment omission in order to break continuous drug pressure on cells and minimize their stressful time periods. Other studies also report the establishment of their DOX-resistant MCF-7 sublines by sequentially treating the cells with concentrations of the drug that ranged from 0.1 to 1 µM.[12,17,18] Christowitz *et al.* further used their resistant sublines to develop a xenograft model.[7] DOX-resistant BC tumors have also been generated *in vivo* by injecting mouse models with the drug at intervals until the tumors grew to a certain volume.[7]

Our generated sublines demonstrated their capacity to maintain resistance to DOX over time. Preliminary analyses indicated that they have a higher growth rate and less apoptosis rate than their DOX-sensitive ancestors. Also, the 25% subline displayed significantly more capacity to migrate compared to control cells. Molecular analyses showed expression alterations in key gene candidates. We found that two of these molecules were bound by DOX with high propensity. Lastly, our 25% subline showed significantly increased CD44:CD24 ratio compared to the control cells, indicating DR and invasive nature of the subline.

The altered expression of multiple gene groups in our resistant subline that we examined significantly supports DOX resistance. The most notable was over 105-fold increase in the mRNA levels of drug metabolizing gene CYP1A1 whose product may support DOX resistance by binding to and inactivating the drug, thereby increasing the rate of cell survival.

ABCB1 and ABCC1, two representatives of ATP-dependent drug transporter genes, were also significantly upregulated in our resistant subline as an indication of reduced intracellular DOX concentration. Mechanistically, the passive diffusion of the hydrophobic DOX molecules and their active efflux from the cell membrane via these transporters prevents nuclear accumulation and activity of DOX,[19] thereby inhibiting DOX-DNA adduct formation and its downstream events that transduce the DNA damage signal into apoptosis.[20] Expression of efflux transporters causes multidrug resistance (MDR) in various cancer types. P-gp encoded by ABCB1 is an important efflux pump that contributes to MDR development.[21] ABCC1 encodes Multidrug Resistance-associated Protein 1 (MRP1) which is involved in MDR by transporting many chemotherapeutic drugs out of cells. ABCC1 overexpression indicates a reduced response to chemotherapeutic drugs and a lower rate of survival.[22] DOX is a substrate for ABCC1, and ABCC1 has already been linked to DOX resistance in MDR cancer cells.[23,24] Lu *et al.* report upregulation of ABCC1 expression at both mRNA and protein levels in their DOX-resistant subline.[21] They also show that over-expression of miR-134 significantly downregulates ABCC1.

The PI3K and AKT1 genes are important components of cell growth signaling pathways and showed overexpression in our resistant subline. While their upregulation supports DOX resistance,[17] inhibition of the components of this signaling pathway using molecular or pharmacological procedures can re-sensitize resistant cancer cells to the drug.[18,25,26]

We observed several folds increase in anti-apoptotic BCL-2 levels and significant reduction in pro-apoptotic BAX levels in our 25% subline. Upregulation of BCL-2 induces DOX resistance, whereas its inhibition restores drug sensitivity.[27-30] Expansion of cancer cell interactions with its extracellular matrix strengthens DOX resistance in correlation with BCL-2 and BCL-XL up-regulation.[27,31]

In our resistant subline, pro-EMT genes SNAIL, STAT3, MMP1 were significantly upregulated, in support of DOX resistance.[32] Downregulation or inactivation of SNAILl and STAT3 breaks cancer cell resistance, and when followed by DOX treatment, prevents xenograft tumor growth.[33,34] In contrast, the 21-folds downregulation of the tumor suppressor gene CDH1 was notable. CDH1encodes E-cadherin which acts as an invasion suppressor.[35] E-cadherin is indeed a crucial cell–cell adhesion molecule that tightens the connection of epithelial cells together. Loss of E-cadherin expression induces EMT and metastasis by triggering the expression of pro-EMT transcription factors (TFs). E-cadherin levels change in EMT and MET and, therefore, the molecule is considered an important switch in EMT.

EMT is an important mechanism of DOX resistance in BC including ER^+ BC. ERα overexpression supports DOX action in E-cadherin downregulation towards EMT and DOX resistance.[36] Therefore, due to ERα presence in MCF-7 cells, frequent DOX treatment of our subline likely downregulated E-cadherin in favor of EMT and increased resistance. Cross-comparison between and $ERα^+$ and $ERα^-$ cell lines suggested that inhibition of ER activity enhances DOX responsiveness in resistant $ERα^+$ BC.[36]

Both TOP2A and TP53 are involved in DNA processing. Over a 100-fold TOP2A downregulation in our resistant subline and a similar report by another study[12] indicates the importance of this enzyme as the prime target of DOX. Overexpression of mutated p53 (TP53) detected in our resistant cells, with modified protein conformation and impairment of p53 activity upon changes in its regulating proteins contributes to DOX resistance.[37]

Our resistant subline expressed several folds higher CCND1 but slightly reduced p21 than did the WT MCF-7. DOX treatment enhances CCND1 expression,[38] whereas suppression of CCND1-encoded cyclin D1 by CDK4 inhibitor reverses DOX resistance and induces apoptosis in MCF-7 cells.[39] Cyclin D1 downregulation by knocking down mTOR/p70S6K in leukemia cells results in cell cycle arrest and apoptosis induction by DOX.[40] DOX activates the expression of cell cycle inhibitors including p21.[41] We presume that p21 downregulation in our cells could have occurred during the acquisition of DOX resistance in our resistant subline.

Our subline expressed several folds less tumor suppressor gene BRCA2 than did the parental MCF-7, similar to a previous report.[12] BRCA2 expression is induced by BRCA1 which supports the response to DOX-induced stress in prostate cancer.[40]

Among the gene groups studied, two candidates displayed profound changes in their expression levels in our resistant subline: CYP1A1 with 106 folds upregulation, and TOP2A with 102 folds downregulation. We simulated DOX binding to either of these two molecules and found that the drug has a strong affinity to bind either molecule, regardless of its net suppressive or inductive effect. According to the literature, some of these molecular changes may have been gained during resistance acquisition and cell adaptation to pressures of drug treatment, whereas others must be considered the outcome of the resistance phenomenon. Given that intracellular pathways are heavily interconnected, it appears from the available reports and our own observations that the candidate genes extensively cross-talk within a network of interconnections, so that early events such as cell survival and growth are shaped by TFs and tumor suppressors before they promote the late events that include DR, EMT, and migration.[42]

SHKN-MTFN co-treatment had important impacts on our DOX-resistant subline. The first change included reduced survival and induced apoptosis. When we increased doses of SHKN and MTFN, survival was diminished in all groups. More importantly, in co-treated groups exposed to DOX, no significant differences were detected in survival between WT cells and our resistant subline implying that DOX and SHKN+MTFN combination synergized to reduce cell survival to a minimum in both WT and resistant cells. Our co-staining experiments indicated that cell death was due to apoptosis and the SHKN-MTFN combination more significantly induced the apoptotic process than did single treatments. Reduced capacity to migrate was the second change. Treatment of cell groups with SHKN stopped cell migration to some extent and, unlike MTFN, the SHKN-treated cells did not show significant movements from 12 hrs to 24 hrs post-scratch. More importantly, SHKN-MTFN co-treatment likely synergized with DOX so that cell migration almost stopped at higher doses of the compounds. The third observation was a reduced CD44/CD24 ratio. The data we generated using flow cytometry indicates that this ratio significantly rose from the drug-sensitive parental cells to our resistant subline. Treatment with SHKN or MTFN significantly reduced the ratio and this reduction was further accelerated in co-treatment samples. Our data indicate that, compared to the untreated resistant control, CD24 populations increased in treated and SHKN-MTFN-co-treated samples. Treatment of wildtype MCF-7 with either drug and particularly with both had significant reducing impact on the CD44/CD24 ratio, as we recently reported too.[13] Despite a significant increase in the ratio observed

during resistance acquisition, single and dual treatments significantly reduced it. In particular, using 11 µM SHKN and 52 mM MTFN (determined as their IC50 when used in combination in our 25% subline), we co-treated our resistant subline populations with three varying doses of the two compounds from sublethal to lethal and achieved between 10 to 16 folds reduction in CD44/CD24 ratios.

The last change we monitored was in the energy of SHKN binding to growth signaling molecules. In our previous study, binding between SHKN, on the one hand, and a number of molecules that contribute to cell signaling pathways, on the other, was simulated and we found favorable binding energy in each case.[13] Table 5 lists these binding energies. SHKN affinity to these molecules is compatible with our observations on cell survival, migration and CSCs markers outlined above. In particular, we made observations similar to DOX, i.e., the energy of SHKN binding to CYP1A1 and TOP2A was found to be high, as it was in the case of DOX. As an anti-resistance mechanism of action, we presumed that SHKN could compete with DOX in binding CYP1A1 towards its downregulation and to TOP2A toward upregulation of this molecule.

CONCLUSION

In conclusion, our current study was carried out to elucidate some of the uncovered cancer cell-drug interactions leading to the process of DOX resistance acquisition and subsequent changes. These findings can be consolidated and improved using stably-made resistant sublines and animal models of various BC subtypes each having distinct characteristics of receptor expression, invasiveness and metastasis. Dissection of such targeted DR models by genome editing and other versatile tools could unravel many mysteries behind DOX resistance. Mechanistic investigations on DR may include the role of chromatin accessibility alterations, TFs and non-coding RNA molecules, followed by downstream developments in gene expression and intracellular tumorigenic pathways. The findings of these steps will be important for efficient re-sensitization of resistant cells by specific DR-targeting measures such as combination of epigenetic therapy and SHKN-MTFN synergy.

ACKNOWLEDGMENT

The authors are thankful to National Institute of Genetic Engineering and Biotechnology (NIGEB) (Grant 708) for funding their research.

ETHICAL CONSIDERATIONS

None required.

CONFLICTS OF INTEREST

There is no conflict of interest between the authors.

FUNDING

This study was financially supported by a grant from National Institute of Genetic Engineering and Biotechnology (NIGEB) (Grant 708).

REFERENCES

1. Vasan N, Baselga J, Hyman DM. A view on drug resistance in cancer. Nature 2019;575:299–309. doi:10.1038/s41586-019-1730-1.
2. Houseman G. Byler S, Heerboth S, Lapinska K, Longacre M, Snyder N, Sarkar S. Drug resistance in cancer: an overview. Cancers (Basel). 2014;6(3):1769-92. doi: 10.3390/cancers6031769.
3. Barrett-Lee PJ, Dixon JM, Farrell C, Jones A, Leonard R, Murray N, Palmieri C, Plummer CJ, Stanley A, Verrill MW. Expert opinion on the use of anthracyclines in patients with advanced breast cancer at cardiac risk. Ann Oncol. 2009;20(5):816-27. doi: 10.1093/annonc/mdn728.
4. "Doxorubicin Hydrochloride". The American Society of Health-System Pharmacists. Doxorubicin Hydrochloride Monograph for Professionals-Drugs.com (archive.org). Retrieved 27 March 2022.
5. Thorn CF, Oshiro C, Marsh S, Hernandez-Boussard T, McLeod H, Klein TE, Altman RB. Doxorubicin pathways: pharmacodynamics and adverse effects. Pharmacogenet Genomics. 2011;21(7):440-6. doi: 10.1097/FPC.0b013e32833ffb56.
6. Early Breast Cancer Trialists' Collaborative Group (EBCTCG). Early Breast Cancer Trialists' Collaborative Group (EBCTCG). Anthracycline-containing and taxane-containing chemotherapy for early-stage operable breast cancer: a patient-level meta-analysis of 100 000 women from 86 randomised trials. Lancet. 2023;401(10384):1277-1292. doi: 10.1016/S0140-6736(23)00285-4.
7. Christowitz C, Davis T, Isaacs A, van Niekerk G, Hattingh S, Engelbrecht AM. Mechanisms of doxorubicin-induced drug resistance and drug resistant tumour growth in a murine breast tumour model. BMC Cancer. 2019;19(1):757. doi: 10.1186/s12885-019-5939-z.
8. Cox J, Weinman S. Mechanisms of doxorubicin resistance in hepatocellular carcinoma. Hepat Oncol. 2016;3(1):57-59. doi:10.2217/hep.15.41.
9. Solazzo M, Fantappie O, D'Amico M et al. Mitochondrial expression and functional activity of breast cancer resistance protein in different multiple drug-resistant cell lines. Cancer Res. 2009;69:7235–7242. doi: 10.1158/0008-5472.CAN-08-4315.

10. Zhang J, Wang Y, Zhen P et al. Genome-wide analysis of miRNA signature differentially expressed in doxorubicin-resistant and parental human hepatocellular carcinoma cell lines. PLoS ONE; 20138(1): e54111. doi: 10.1371/journal.pone.0054111.
11. Kubiliūtė R, Šulskytė I, Daniūnaitė K, Daugelavičius R, Jarmalaitė S. Molecular features of doxorubicin-resistance development in colorectal cancer CX-1 cell line. Medicina (Kaunas). 2016;52(5):298-306. doi: 10.1016/j.medici.2016.09.003.
12. AbuHammad S, Zihlif M. Gene expression alterations in doxorubicin resistant MCF7 breast cancer cell line. Genomics. 2013;101(4):213-20. doi: 10.1016/j.ygeno.2012.11.009.
13. Gardaneh M, Shojaei S, Kaviani A, Behnam B GDNF induces RET-SRC-HER2-dependent growth in trastuzumab-sensitive but SRC-independent growth in resistant breast tumor cells. Breast Cancer Res Treat. Breast Cancer Res Treat. 2017;162(2):231-241. doi: 10.1007/s10549-016-4078-3.
14. Livak KJ, Schmittgen TD (2001) Analysis of relative gene expression data using real-time quantitative PCR and the 2−ΔΔCT method. Methods;25(4):402-8.doi: 10.1006/meth.2001.1262.
15. Rostamian Tabari A, Gavidel P, Sabouni F, Gardaneh M (2022) Synergy between sublethal doses of shikonin and metformin fully inhibits breast cancer cell migration and reverses epithelial-mesenchymal transition. Mol Biol Rep. 2022:49(6):4307-4319. doi: 10.1007/s11033-022-07265-9. Epub 2022 May 7.
16. Dagogo-Jack, I., Shaw, A. Tumour heterogeneity and resistance to cancer therapies. Nat Rev Clin Oncol;15(2):81–94. Doi:10.1038/nrclinonc.2017.166.
17. Yang CL, Jiang FQ, Xu F, Jiang GX. ADAM10 overexpression confers resistance to doxorubicin-induced apoptosis in hepatocellular carcinoma. Tumour Biol. 2012;33(5):1535-41. doi: 10.1007/s13277-012-0405-4.
18. Chen JM, Bai JY, Yang KX. Effect of resveratrol on doxorubicin resistance in breast neoplasm cells by modulating PI3K/Akt signaling pathway. IUBMB Life. 2018;70(6):491-500. doi: 10.1002/iub.1749.
19. Aminipour Z, Khorshid M, Keshvari H, Bonakdar S, Wagner P, Van der Bruggen B. Passive permeability assay of doxorubicin through model cell membranes under cancerous and normal membrane potential conditions. Eur J Pharm Biopharm. 2020;146:133-142. doi: 10.1016/j.ejpb.2019.10.011.
20. Forrest RA, Swift LP, Rephaeli A, Nudelman A, Kimura K, Phillips DR, Cutts SM. Activation of DNA damage response pathways as a consequence of anthracycline-DNA adduct formation. Biochem Pharmacol. 2012;15;83(12):1602-12. doi: 10.1016/j.bcp.2012.02.026.
21. Lu L, Ju F, Zhao H, Ma X. MicroRNA-134 modulates resistance to doxorubicin in human breast cancer cells by downregulating ABCC1. Biotechnol Lett. 2015;37(12):2387-94. doi: 10.1007/s10529-015-1941-y.
22. Munoz M, Henderson M, Haber M, Norris M. Role of the MRP1/ABCC1 multidrug transporter protein in cancer. IUBMB Life. 2007;59(12):752-7. doi: 10.1080/15216540701736285.
23. Bonhoure E, Pchejetski D, Aouali N, Morjani H, Levade T, KohamaT, Cuvillier O. Overcoming MDR-associated chemoresistance in HL-60 acute myeloid leukemia cells by targeting sphingosine kinase-1. Leukemia. 2006;20(1):95-102. doi: 10.1038/sj.leu.2404023.
24. Angelini A, Ciofani G, Baccante G, Di Febbo C, Carmine DI, Cuccurullo F, Porreca E. Modulatory effects of heparin on cellular accumulation and cytotoxicity of doxorubicin in MRP1-overexpressing HL60/doxo cells. Anticancer Res 2007;27(1A):351-5.
25. Li Y, Ye Y, Feng B, Qi Y. Long Noncoding RNA lncARSR Promotes Doxorubicin Resistance in Hepatocellular Carcinoma via Modulating PTEN-PI3K/Akt Pathway. J Cell Biochem. 2017;118(12):4498-4507. doi: 10.1002/jcb.26107.
26. Jung KA, Choi BH, Kwak MK. The c-MET/PI3K signaling is associated with cancer resistance to doxorubicin and photodynamic therapy by elevating BCRP/ABCG2 expression. Mol Pharmacol. 2015;87(3):465-76. doi: 10.1124/mol.114.096065.
27. Ugarenko M, Nudelman A, Rephaeli A, Kimura K, Phillips DR, Cutts SM. ABT-737 overcomes Bcl-2 mediated resistance to doxorubicin-DNA adducts. Biochem Pharmacol. 2010;79(3):339-49. doi: 10.1016/j.bcp.2009.09.004.
28. van Oosterwijk JG, Herpers B, Meijer D, Briaire-de Bruijn IH, Cleton-Jansen AM, Gelderblom H, van de Water B, Bovée JV. Restoration of chemosensitivity for doxorubicin and cisplatin in chondrosarcoma in vitro: BCL-2 family members cause chemoresistance. Ann Oncol. 2012;23(6):1617-26. doi: 10.1093/annonc/mdr512.
29. Sun W, Chen X, Xie C, Wang Y, Lin L, Zhu K, Shuai X. Co-Delivery of Doxorubicin and Anti-BCL-2 siRNA by pH-Responsive Polymeric Vector to Overcome Drug Resistance in In Vitro and In Vivo HepG2 Hepatoma Model. Biomacromolecules. 2018;19(6):2248-2256. doi: 10.1021/acs.biomac.8b00272.
30. Zhao Y, Zhang CL, Zeng BF, Wu XS, Gao TT, Oda Y. Enhanced chemosensitivity of drug-resistant osteosarcoma cells by lentivirus-mediated Bcl-2 silencing. Biochem Biophys Res Commun. 2009;390(3):642-7. doi: 10.1016/j.bbrc.2009.10.020.
31. Lovitt CJ, Shelper TB, Avery VM. Doxorubicin resistance in breast cancer cells is mediated by extracellular matrix proteins. BMC Cancer. 2018;18(1):41. doi:10.1186/s12885-017-3953-6.
32. Shen CJ, Kuo YL, Chen CC, Chen MJ, Cheng YM. MMP1 expression is activated by Slug and enhances multi-drug resistance (MDR) in breast cancer. PLoS One. 2017;12(3):e0174487. doi: 10.1371/journal.pone.0174487.
33. Yang X, Shang P, Yu B, Jin Q, Liao J, Wang L, Ji J, Guo X. Combination therapy with miR34a and doxorubicin synergistically inhibits Dox-resistant breast cancer progression via down-regulation of Snail through suppressing Notch/NF-κB and RAS/RAF/MEK/ERK signaling pathway. Acta Pharm

Sin B. 2021;11(9):2819-2834. doi: 10.1016/j.apsb.2021.06.003.
34. Gariboldi MB, Ravizza R, Molteni R, Osella D, Gabano E, Monti E. Inhibition of Stat3 increases doxorubicin sensitivity in a human metastatic breast cancer cell line. Cancer Lett. 2007;258(2):181-8. doi: 10.1016/j.canlet.2007.08.019.
35. Polyak K, Weinberg RA. Transitions between epithelial and mesenchymal states: acquisition of malignant and stem cell traits. Nat Rev Cancer. 2009;9(4):265-73. doi: 10.1038/nrc2620.
36. Wan X, Hou J, Liu S, Zhang Y, Li W, Zhang Y, Ding Y. Estrogen Receptor α Mediates Doxorubicin Sensitivity in Breast Cancer Cells by Regulating E-Cadherin. Front Cell Dev Biol. 2021 Feb 4;9:583572. doi: 10.3389/fcell.2021.583572.
37. Hientz K, Mohr A, Bhakta-Guha D, Efferth T. The role of p53 in cancer drug resistance and targeted chemotherapy. Oncotarget. 2017;8(5):8921-8946. doi:10.18632/oncotarget.13475.
38. Zuryń A, Litwiniec A, Klimaszewska-Wiśniewska A, Nowak JM, Gackowska L, Myśliwiec BJ, Pawlik A, Grzanka A. Expression of cyclin D1 after treatment with doxorubicin in the HL-60 cell line. Cell Biol Int. 2014;38(7):857-67. doi: 10.1002/cbin.10290.
39. Tarasewicz E, Hamdan R, Straehla J, Hardy A, Nunez O, Zelivianski S, Dokic D, Jeruss JS. CDK4 inhibition and doxorubicin mediate breast cancer cell apoptosis through Smad3 and survivin. Cancer Biol Ther. 2014;15(10):1301-11. doi: 10.4161/cbt.29693.
40. Li J, Liu W, Hao H, Wang Q and Xue L: Rapamycin enhanced the antitumor effects of doxorubicin in myelogenous leukemia K562 cells by downregulating the mTOR/p70S6K pathway. Oncol Lett. 2019;18(3):2694-2703. doi: 10.3892/ol.2019.10589.
41. Denard B, Lee C, Ye J. Doxorubicin blocks proliferation of cancer cells through proteolytic activation of CREB3L1. Elife. 2012;1:e00090. doi: 10.7554/eLife.00090.
42. Huilgol D, Venkataramani P, Nandi S, Bhattacharjee S. Transcription Factors That Govern Development and Disease: An Achilles Heel in Cancer. Genes (Basel). 2019;10(10):794. doi: 10.3390/genes10100794.

How to Cite This Article

Keshandehghan A, Rostamian Tabari A, Panahi Y, Gardaneh M. Acquisition of Doxorubicin Resistance Induces Breast Cancer Cell Migration and Epithelial-Mesenchymal Transition that are Reversed by Shikonin-Metformin Synergy. Arch Breast Cancer. 2024; 11(2):159-71.
Available from: https://www.archbreastcancer.com/index.php/abc/article/view/891